Progress In Electromagnetics Research B, Vol. 103, 159–176, 2023

Compact Multiband High-Gain Millimeter-Wave Planar Antenna

Asmaa E. Farahat and Khalid F. A. Hussein*

Abstract—A novel miniaturized high-gain Vivaldi antenna printed on a thin substrate is proposed for operation as a multi-band antenna for millimeter-wave applications. The present work proposes a novel geometrical design of the Vivaldi antenna that is printed on the opposite faces of a thin dielectric substrate. The antenna has compact size, and its dimensions are optimized to enhance the performance regarding the bandwidth of impedance matching, gain, and radiation efficiency. To maximize the gain within a desired frequency band, each arm of the Vivaldi antenna is loaded by a ring-shaped parasitic element. The results of the parametric study for antenna design optimization regarding the enhancement of the impedance matching bandwidth and the antennas gain are presented and discussed. Also, it is shown through parametric study that the size and location of the parasitic rings can be optimized to enhance the antenna gain over the desired frequency range. The multiband operation of the proposed Vivaldi antenna is explained in view of the multimode operation that is illustrated by the distributions of the surface current on the antenna arms and the electric field in tapered slot. A novel microstrip line/parallel-strip line balun structure is proposed for feeding the balanced Vivaldi antenna and to achieve wideband impedance matching. The proposed Vivaldi antenna is fabricated and subjected to performance evaluation through measurements. It is shown that the antenna impedance is matched to 50 Ω over the four frequency bands: 22.0–27.7 GHz, 32.0–37.5 GHz, 41.5–46.6 GHz, and 51.7–56.7 GHz. The corresponding bandwidths are 5.7, 5.5, 5.1, and 5.0 GHz, respectively with percent bandwidths of 23%, 16%, 11.6%, and 9.2%, respectively. In spite of its compact size, the achieved values of the maximum gain are 6 dBi, 9 dBi, 11.4 dBi, and 12 dBi over the mentioned frequency bands, respectively. Also, the corresponding values of radiation efficiency are 98%, 97%, 95%, and 93%, respectively. The proposed Vivaldi antenna is fabricated and subjected to measurement for experimental investigation of its performance. The measurement shows good agreement with the simulation results.

1. INTRODUCTION

Recently, researchers have been attracted to the millimeter wave (mm-wave) band that refers to the frequency spectrum 30–300 GHz. Using the mm-wave range in communications can allow high speed, low latency, and very high data rates of many Gbps. Leading applications such as the high definition (HD) televisions and HD videos, automotive, satellite and 5G mobile communications, and virtual reality benefit from the large bandwidth and high data rates offered by the mm-wave frequency spectrum [1]. Due to the small wavelength, antennas in mm-wave range occupy smaller space because of their small size which allows to design antenna arrays with enhanced performance and higher gain in a limited area [2]. Higher bands of 5G (24–47 GHz) and Ka-band (27–40 GHz) used in satellite communications require high gain antennas to overcome the atmospheric attenuation due to water vapor absorption and propagation path loss at these frequency bands [3]. Also, high gain antennas are important for microwave imaging systems, radar, GPR detection, remote sensing, as well as medical field [4].

Received 6 August 2023, Accepted 27 October 2023, Scheduled 13 November 2023
* Corresponding author: Khalid Fawzy Ahmed Hussein (fkhalid@eri.sci.eg).
The authors are with the Electronics Research Institute (ERI), Cairo 11843, Egypt.

Antipodal Vivaldi antennas have been invented to improve the gain and bandwidth in the high frequency applications [5–7]. The antipodal Vivaldi has been introduced in [6]. Many researches then have been conducted to improve the performance of the Vivaldi antenna regarding the size reduction, impedance matching bandwidth, and improved radiation characteristics. For example, in [8], a compact high gain antipodal Vivaldi antenna is implemented for 5G applications using negative metamaterial. The unit cells of the metamaterial are arranged between two arms of the Vivaldi antenna in order to transfer all energy in the end-fire direction. This antenna achieves a gain that varies between 11 and 13.5 dB over the operating band 24–30 GHz. In [9], an antipodal Vivaldi antenna with improved radiation performance at high-frequency band is proposed with a double asymmetric trapezoidal parasitic patch added to the aperture of the antenna. The antenna operates in the frequency range 6–26.5 GHz with a gain of 9 dBi. The concept of adding parasitic patch has also been used in [10] to enhance the radiation in the end-fire direction to increase the achieved gain to about 10 dB in the frequency band 6–21 GHz but with a total size of 140 mm × 66 mm × 1.5 mm. An antipodal Vivaldi antenna with regular slot edges to improve the start low frequency and adding a loaded lens at the flare ends to enhance the end high frequency of the operating band has been investigated in [11]. The antenna achieves a wide frequency band 4–30 GHz but with low gain of 5 dBi. Some recently published work proposes planar Vivaldi antennas for multiband operation such as those presented in [12–19].

In this work, a novel method is introduced for constructing the Vivaldi antenna arms. This method is based on the extraction of an area that is subtended between two ellipses; the outer ellipse forms the edge of the tapered slot of the Vivaldi antenna. The two arms of the antenna are printed on the opposite faces of the dielectric substrate. The feed line is a microstrip line printed on the top face of the substrate and connected to the right arm of the antenna. A microstrip line/parallel-strip line balun structure is proposed for feeding the balanced Vivaldi antenna and to achieve wideband impedance matching. The ground plane is printed on the bottom surface of the substrate and is connected to the left arm of the antenna. The feeding microstrip line is connected to the two-arm antenna through a twins-waveguide region for impedance matching. Each arm of the antenna is loaded by a conducting ring through a semicircular slot for gain enhancement. The multiband operation of the proposed Vivaldi antenna is explained in view of the multimode operation that is illustrated by the distributions of the surface current on the antenna arms and the electric field in tapered slot.

The following presentations of the present article are organized through seven sections. Section 2 describes the antenna design. Section 3 presents a parametric study for the optimum antenna design. Section 4 describes the fabricated model of the antenna. Section 5 explains the experimental work. Section 6 provides presentations and discussions of the simulation results. Section 7 presents comparisons with other published work. The conclusions are summarized in Section 8.

2. ANTENNA DESIGN

The Vivaldi antenna can be described as a radiating tapered slot whose width increases while moving away from the feeding point. This antenna has two coplanar conducting surfaces on the sides of the tapered slot which, theoretically, have infinite extensions in the transvers direction to the slot axis. If these side planes are truncated in the transverse direction, they can be considered at two arms of the coplanar antenna structure. A novel method for realizing such a Vivaldi antenna with truncated side planes is illustrated in Figure 1. Each of the antenna arms can be constructed by two ellipses as shown in Figure 1. The outer ellipse has its major and minor axes of lengths a_v and a_h, respectively, whereas the inner ellipse has its major and minor axes of lengths b_h and b_v, respectively. The inner ellipse has its major axis coincident with the minor axis of the outer ellipse, and both of them are coincident with the x-axis. The center points of the two ellipses are shifted by X_S in the x-direction. In this geometry, each arm has four boundaries: the outer ellipse, inner ellipse, horizontal x-axis, and truncating the straight line that lies at a distance W_A from the y-axis and parallel to it. In this way, the shaded part shown in Figure 1 can be extracted as one of Vivaldi antenna arms whereas the other arm is a mirror of it, where the mirror plane contains the centerline of the tapered slot and is perpendicular to the antenna plane.

The method of constructing the Vivaldi antenna arms is applied, and the proposed antenna structure can be built as shown in Figure 2. The two arms of the antenna are printed on the opposite faces of the dielectric substrate. The feed line is a microstrip line printed on the top face of the substrate

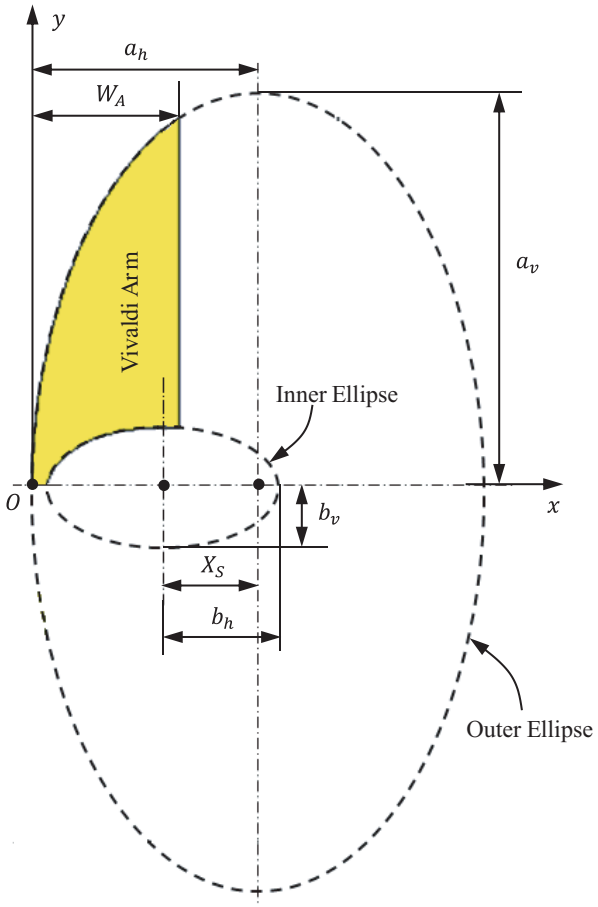

Figure 1. Geometrical boundaries of one arm of the proposed Vivaldi antenna.

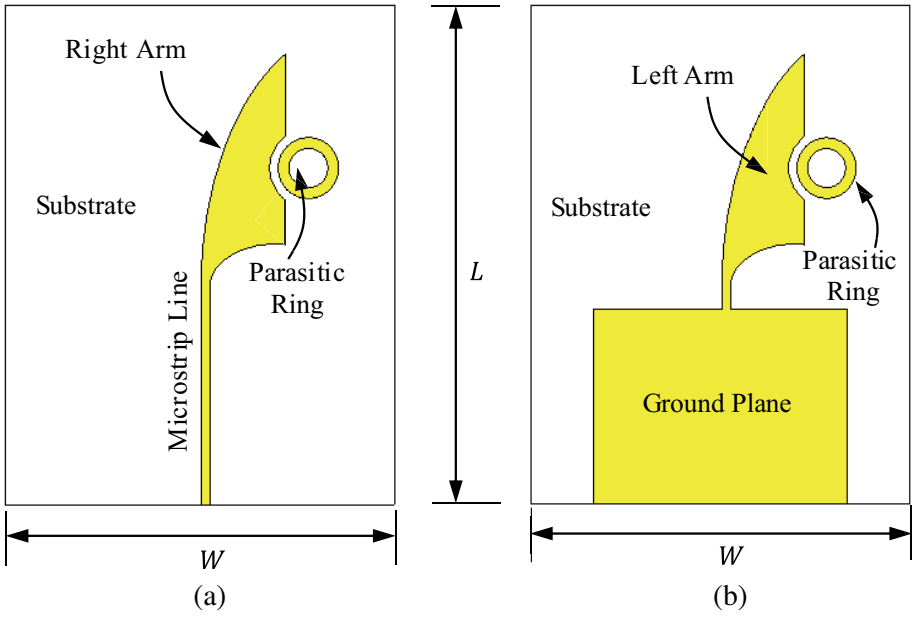

Figure 2. The printed Vivaldi antenna with the parasitic rings. (a) Top view (right arm of the antenna). (b) Bottom view (left arm of the antenna).

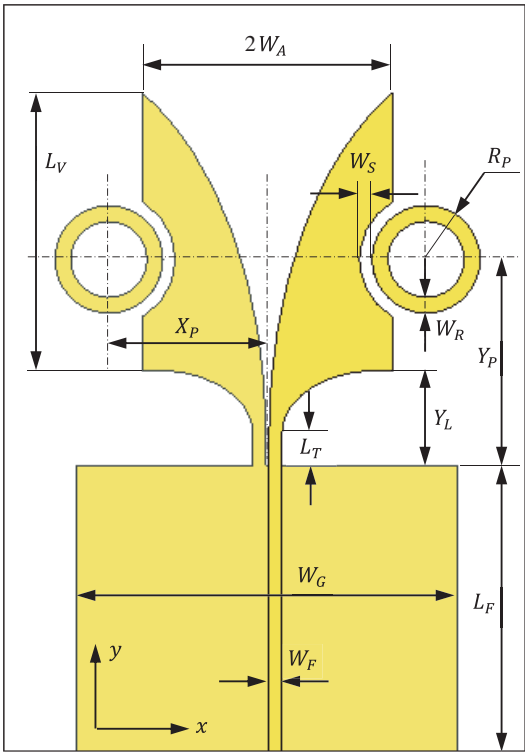

Figure 3. Top view with transparent substrate showing the complete design parameters of the proposed high-gain Vivaldi antenna.

and connected to the right arm of the antenna. The ground plane is printed on the bottom surface of the substrate and is connected to the left arm of the antenna. The feeding microstrip line is connected to the two-arm antenna through a twins-waveguide region for impedance matching. Each arm of the antenna is loaded by a conducting ring through a semicircular slot for gain enhancement.

The antenna design described above results in a Vivaldi antenna that can operate in multiple wide bands of the frequency. The multiband operation of the proposed Vivaldi antenna can be explained as follows. In a tapered slot structure with side conducting surfaces of infinite side extension, broadband radiation will be obtained. When the side conductors are truncated to a finite length, the radiating structure combines multi-resonance (multi-mode) and broadband characteristics in one structure to result in multiple resonating bands, each of which is broadband. The center frequency and span of each band depend on the dimensions and shape of the tapered-slot structure.

The design parameters of the novel Vivaldi antenna are presented in Figure 3 where the bottom layer is seen through the substrate just for illustration. The feeding microstrip line is connected to the two-arm antenna through a parallel-twins transmission line region of length L_T that can be set to allow impedance matching over the desired frequency band. This antenna is printed on a thin flexible dielectric substrate of type Rogers' RO3003 with dielectric constant $\epsilon_r = 3.0$, loss tangent $\delta = 0.001$, and thickness $h = 0.25\,\text{mm}$. The optimum performance of the Vivaldi antenna presented in Figure 3 regarding the frequency band of impedance matching and the maximum gain is obtained when the design parameters are set as listed in Table 1. It should be noted that the dimensions listed in Table 1 are obtained through numerical investigations by the CST® simulator to perform parametric study. Some examples of these parametric studies are presented and discussed in Section 3 of the present work.

3. PARAMETRIC STUDY FOR OPTIMUM ANTENNA DESIGN

This section is concerned with demonstrating some examples of parametric study to determine the best values of the dimensional parameters (listed in Table 1) for the optimal design of the proposed multiband

Table 1. Dimensions of the multiband high-gain Vivaldi antenna of the design presented in Figure 2.

Parameter	W	L	h	a_h	a_v	b_h	b_v	X_S	W_A
Value (mm)	17.9	23	0.25	7	12	3	2	3	3.65
Parameter	R_P	W_R	W_S	X_P	Y_P	L_T	L_F	W_F	W_G
Value (mm)	1.2	0.5	0.4	4.5	5.5	0.45	10	0.4	12

Vivaldi antenna. The design of this antenna has two main objectives. One of the design objectives is to obtain the widest possible frequency band over which the antenna impedance is matched to 50 Ω. The other design objective is to maximize the antenna gain especially for the millimeter-wave bands of the antenna operation.

3.1. Parametric Study for Impedance Matching

The edge of the tapered slot of the Vivaldi antenna is formed using the outer ellipse as described in Section 2 and illustrated in Figure 1. The length a_v of the major axis of the outer ellipse has a major effect on the impedance matching of the Vivaldi antenna. Figure 4 presents the effect of changing a_v on the frequency response of $|S_{11}|$. It is shown that the proposed Vivaldi antenna has four bands over which the impedance is matched to 50 Ω. For $a_v = 8$ mm, the antenna has only three bands of impedance matching. It is clear that the widest frequency band at each of the four bands is obtained when $a_v = 12$ mm.

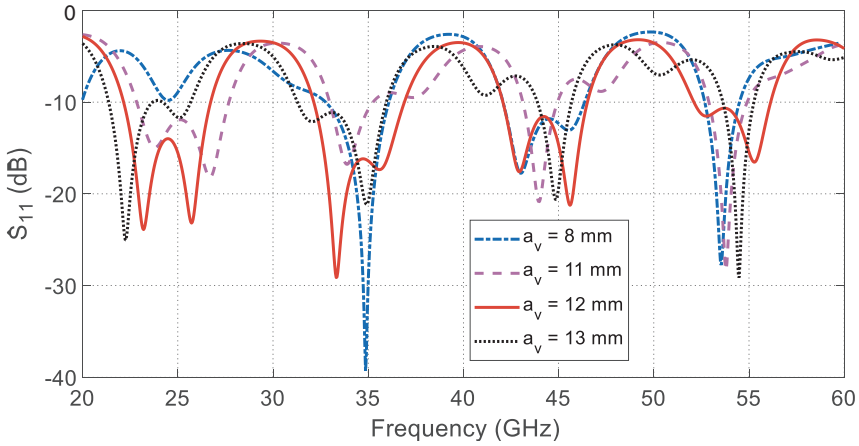

Figure 4. Variation of $|S_{11}|$ (at the antenna feeding port) with varying the frequency for different values of the dimension a_v. The other dimensions of the antenna are listed in Table 1.

Each arm of the Vivaldi antenna has the width W_A as described in Section 2 and illustrated in Figures 1 and 3. This dimension has a major effect on the impedance matching of the Vivaldi antenna. The frequency response of $|S_{11}|$ for different values of W_A is shown in Figure 5. It is shown that the widest frequency band at each of the four bands of the Vivaldi antenna is obtained when $W_A = 3.65$ mm.

As described in Section 2 and illustrated in Figures 2 and 3, two parasitic rings are capacitively coupled to the antenna arms to improve the performance of the proposed Vivaldi antenna. The size of the parasitic ring is mainly determined by the outer radius, R_P, whereas its location is determined by the dimensions, X_P and Y_P. It is required to investigate the effects of the three parameters R_P, X_P, and Y_P on the impedance matching bandwidth as well as the maximum antenna gain. As shown in Figures 6, 7, and 8, the three parameters have minor effects on the impedance matching over the four frequency bands of the proposed Vivaldi antenna. However, in the next section, it is shown that these parameters have major effects on the far-field parameters and can be optimized to enhance the maximum gain obtained by the Vivaldi antenna.

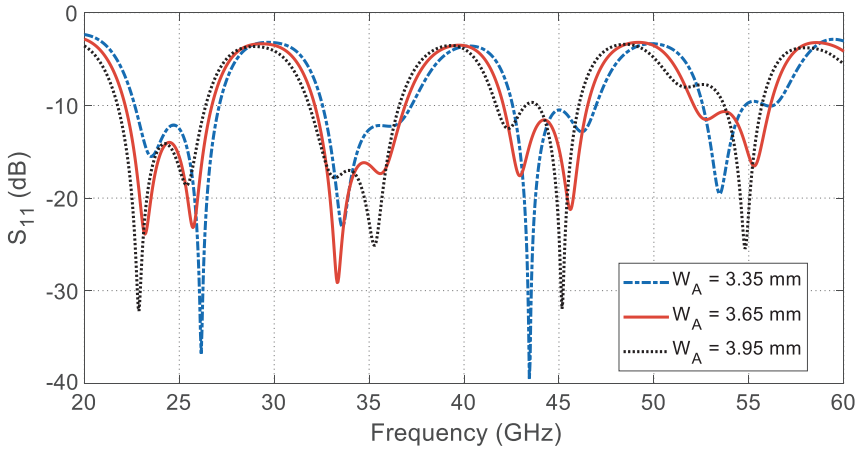

Figure 5. Variation of $|S_{11}|$ (at the antenna feeding port) with varying the frequency for different values of the dimension W_A. The other dimensions of the antenna are listed in Table 1.

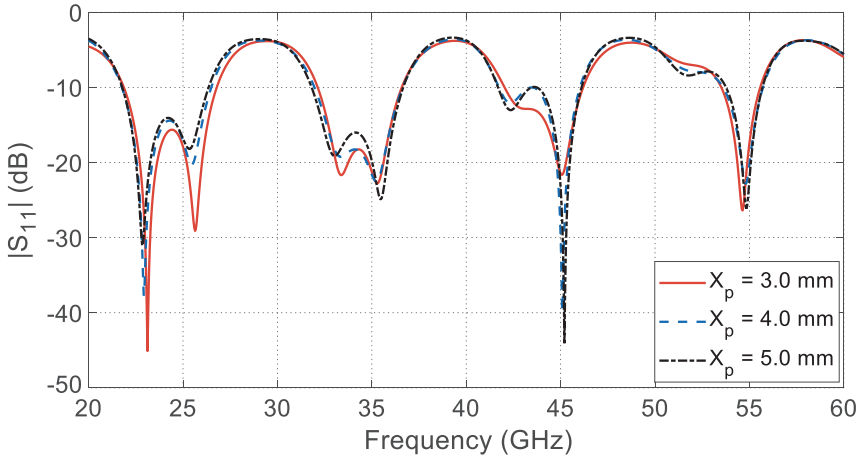

Figure 6. Effect of the ring horizontal location X_P on the reflection coefficient of the proposed Vivaldi antenna. The other dimensions of the antenna are listed in Table 1.

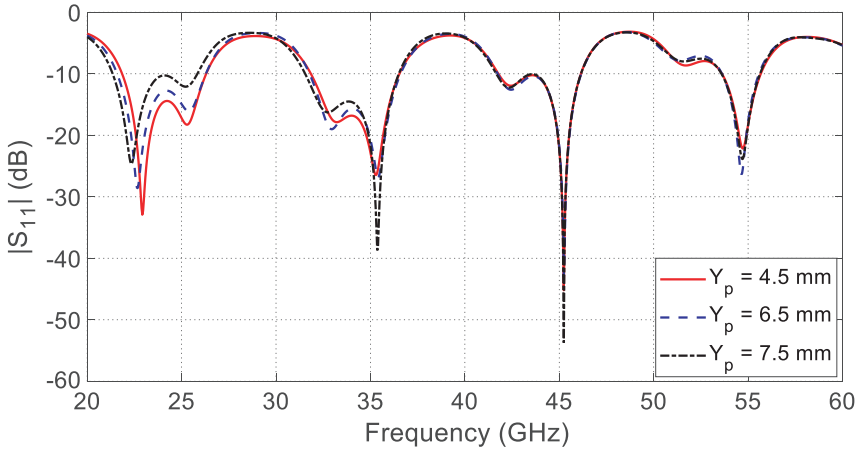

Figure 7. Effect of the ring vertical location Y_P on the reflection coefficient of the proposed Vivaldi antenna. The other dimensions of the antenna are listed in Table 1.

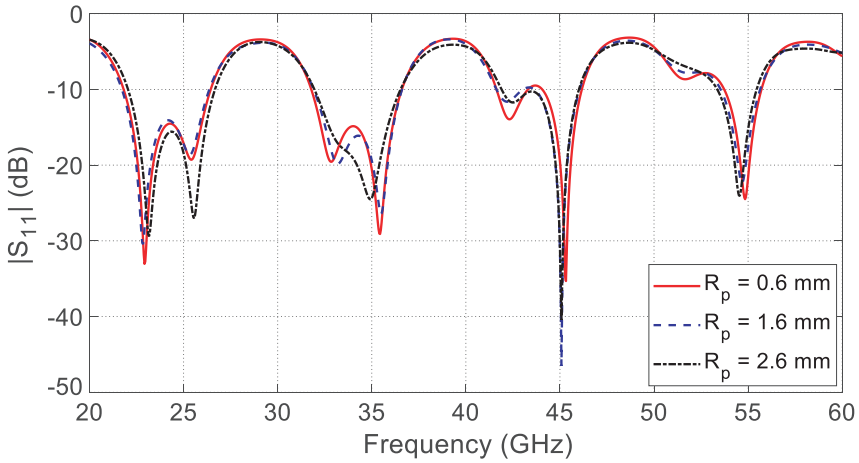

Figure 8. Effect of the ring radius R_P on the reflection coefficient of the proposed Vivaldi antenna. The other dimensions of the antenna are listed in Table 1.

3.2. Parametric Study for Gain Maximization

As discussed in Section 3.1, the dimensional parameters R_P, X_P, and Y_P determining the size and position of the parasitic rings that are capacitively coupled to the antenna arms have minor effects on the impedance matching over the four frequency bands of the proposed Vivaldi antenna. The purpose of loading the arms of the proposed Vivaldi antenna by these parasitic rings is to enhance the maximum gain. The parasitic ring size is mainly determined by the outer radius, R_P, whereas its location is determined by the dimensions, X_P and Y_P. The three dimensional parameters R_P, X_P, and Y_P can be optimized to maximize the gain over a given frequency range.

Due to the semi-circular slot between the arm and the ring, the coupling between them is capacitive. This means that at some given frequency the capacitive loading of the ring on the antenna arm will produce a maximum current on the antenna surface thereby leading to enhancing the maximum gain of the antenna. The same applies to the location of the parasitic ring relative to the antenna arm. For increasing the coupling between the arm and the ring, the horizontal location, X_P, can be decreased for more penetration of the ring inside the arm area. This means that changing X_P results in changing the load of the rings on the antenna arms. Thus, at a specific value of X_P, the coupling load of the ring will maximize the current flowing on the ring thereby maximizing the gain at the operating frequency.

In this section, the effects of three parameters R_P, X_P, and Y_P on the antenna gain are investigated. As the proposed Vivaldi antenna can be considered as high-gain antenna over the third and fourth frequency bands, the effects of these parameters on the antenna gain near the center frequencies of the third and fourth frequency bands are investigated, and their optimum values that give the maximum gain at 45 GHz and 55 GHz (as examples) are determined. It should be noted that while the values of the dimensional parameters under investigation are changed for parametric study, the other dimensions are those listed in Table 1.

3.2.1. Parametric Study for Gain Maximization over the Third Frequency Band

The effect of changing the outer radius, R_P, of the parasitic ring on the maximum antenna gain at 45 GHz is depicted in Figure 9(a). It is shown that the maximum gain is obtained when $R_P = 1.2$ mm. This can be interpreted as that when $R_P = 1.2$ mm, the load impedance of the rings on the antenna arms at 45 GHz reaches a value that causes the magnitude of the surface current flowing on the antenna arms and on the rings to be increased and thereby enhancing the radiated field in the far zone and increasing the antenna gain. This will be presented and discussed in Section 4.1. It is shown in Figure 9(b) that $X_p = 4.5$ mm results in the maximum gain of the antenna. In a similar manner, the vertical location Y_p of the ring relative to the antenna arm affects the load of coupling, thereby affecting the ring current and the gain. The maximum gain is obtained when $Y_p = 5.5$ mm as shown in Figure 9(c).

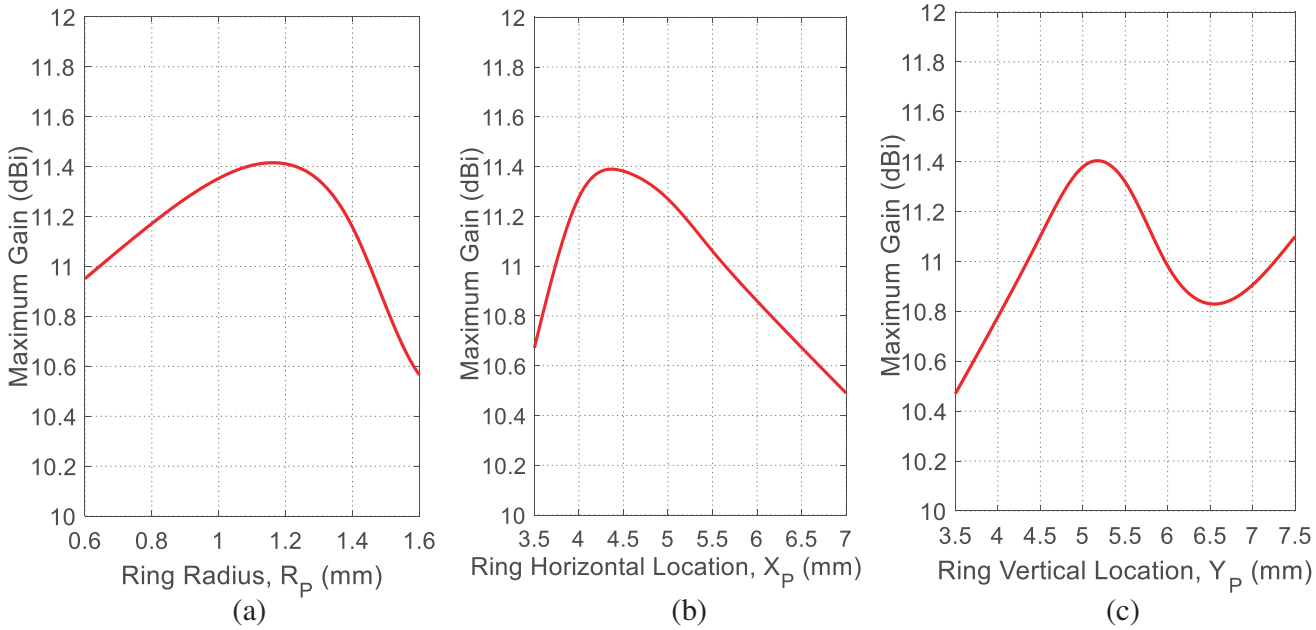

Figure 9. Dependence of the maximum gain of the proposed Vivaldi antenna on the radius and location of the parasitic ring at 45 GHz.

3.2.2. Parametric Study for Gain Maximization over the Fourth Frequency Band

The effect of changing the outer radius, R_P, of the parasitic ring on the maximum antenna gain at 55 GHz is depicted in Figure 10(a). It is shown that the maximum gain is obtained when $R_P = 1.5$ mm. This can be interpreted as that when $R_P = 1.5$ mm, the load impedance of the rings on the antenna arms at 55 GHz reaches a value that causes the magnitude of the surface current flowing on the antenna

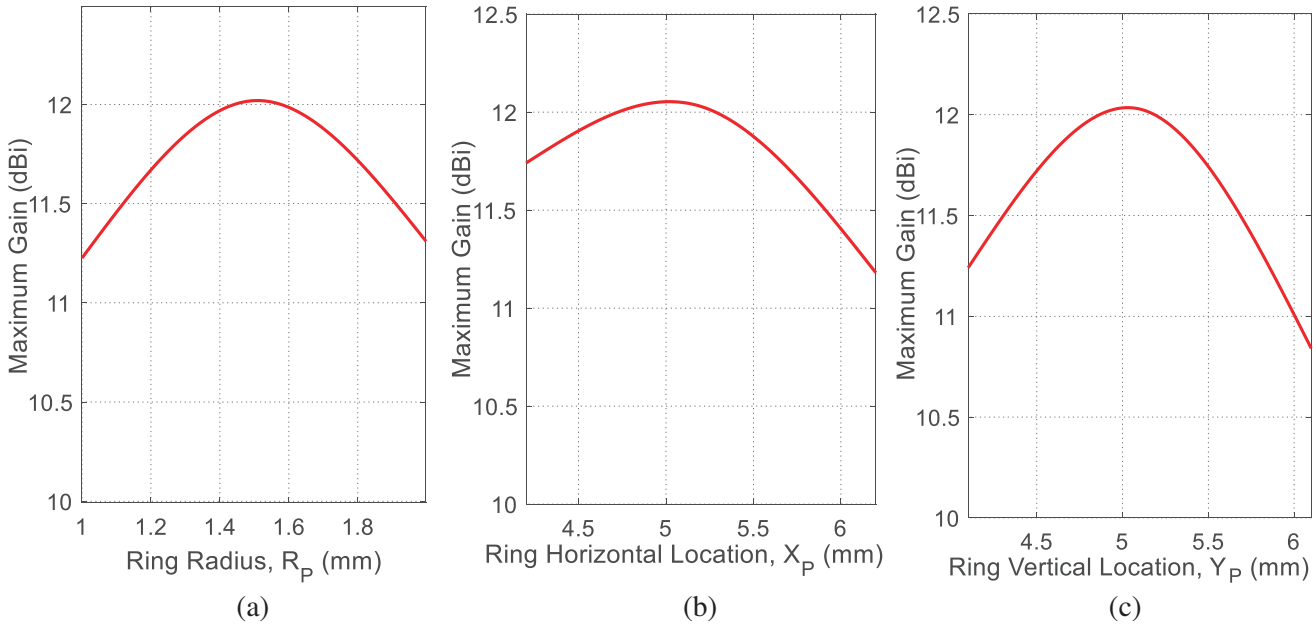

Figure 10. Dependence of the maximum gain of the proposed Vivaldi antenna on the radius and location of the parasitic ring at 55 GHz.

arms and on the rings to be increased and thereby enhancing the antenna gain. Figure 10(b) shows that $X_P = 5.2\,\text{mm}$ results in the maximum gain of the antenna. In a similar manner, the vertical location Y_P of the ring relative to the antenna arm affects the load of coupling, thereby affecting the ring current and the gain. The maximum gain is obtained when $Y_P = 5.1\,\text{mm}$ as shown in Figure 10(c).

4. NEAR FIELD AND SURFACE CURRENT DISTRIBUTION

This section is concerned with the explanation of the multiband operation of the proposed Vivaldi antenna though the presentation of the surface current distribution especially on the conducting antenna arms and the electric field distribution especially in the tapered slot. It may be worthwhile to mention that these distributions are obtained through the CST® simulator.

4.1. Current Distribution

For understanding the multiband operation of the proposed Vivaldi antenna that is based on multimode operation, the current distributions on the conducting surfaces of the proposed Vivaldi antenna near

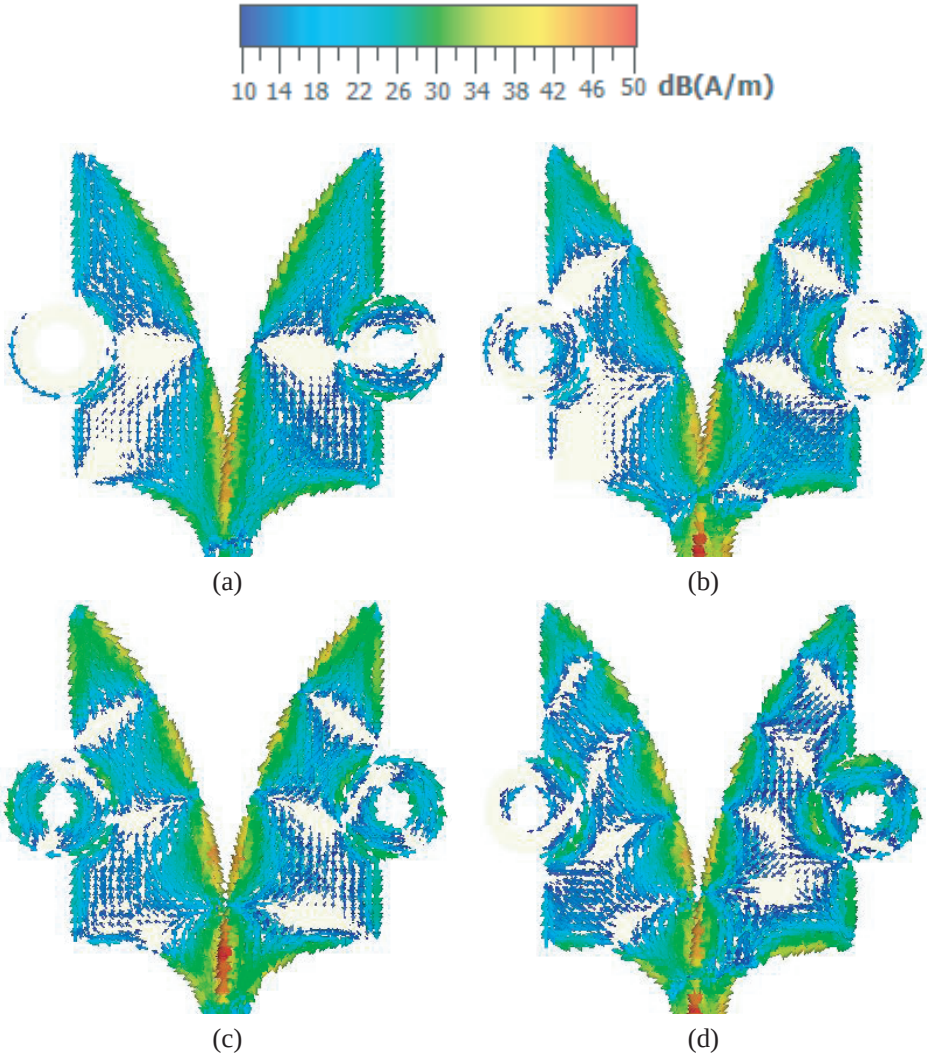

Figure 11. Current distributions on the surface of the Vivaldi antenna arms near the center frequencies of the four bands: (a) 25 GHz, (b) 35 GHz, (c) 45 GHz, and (d) 55 GHz. The dimensions of the antenna are listed in Table 1.

the center frequencies of the four operable frequency bands are presented as shown in Figure 11. It is shown that surface current patterns exhibit modal distributions with increasing order modes (first-order at 25 GHz, second-order at 35 GHz, third-order at 45 GHz, and fourth-order at 55 GHz). Also, it is clear that when $R_P = 1.2$ mm the magnitude of the surface current flowing on the antenna arms and on the rings is increased at 45 GHz as shown in Figure 11(c) in comparison to the surface current distribution at the other frequencies. This can be interpreted as that when $R_P = 1.2$ mm the load impedance of the rings on the antenna arms at 45 GHz reaches a value that enhances the magnitude of the surface current at this frequency thereby leading to enhancing the radiated field in the far zone and increasing the antenna gain.

4.2. Electric Field Distribution in the Tapered Slot

For more understanding of the multiband operation of the proposed Vivaldi antenna that is based on multimode operation, the electric field distributions in the tapered slot of the proposed Vivaldi antenna near the center frequencies of the four operable frequency bands are presented in Figure 12. It is shown that the electric field distribution in the tapered slot emphasizes the same concept of multimode operation that results in multiband operation of the finite-length tapered slot antenna structure.

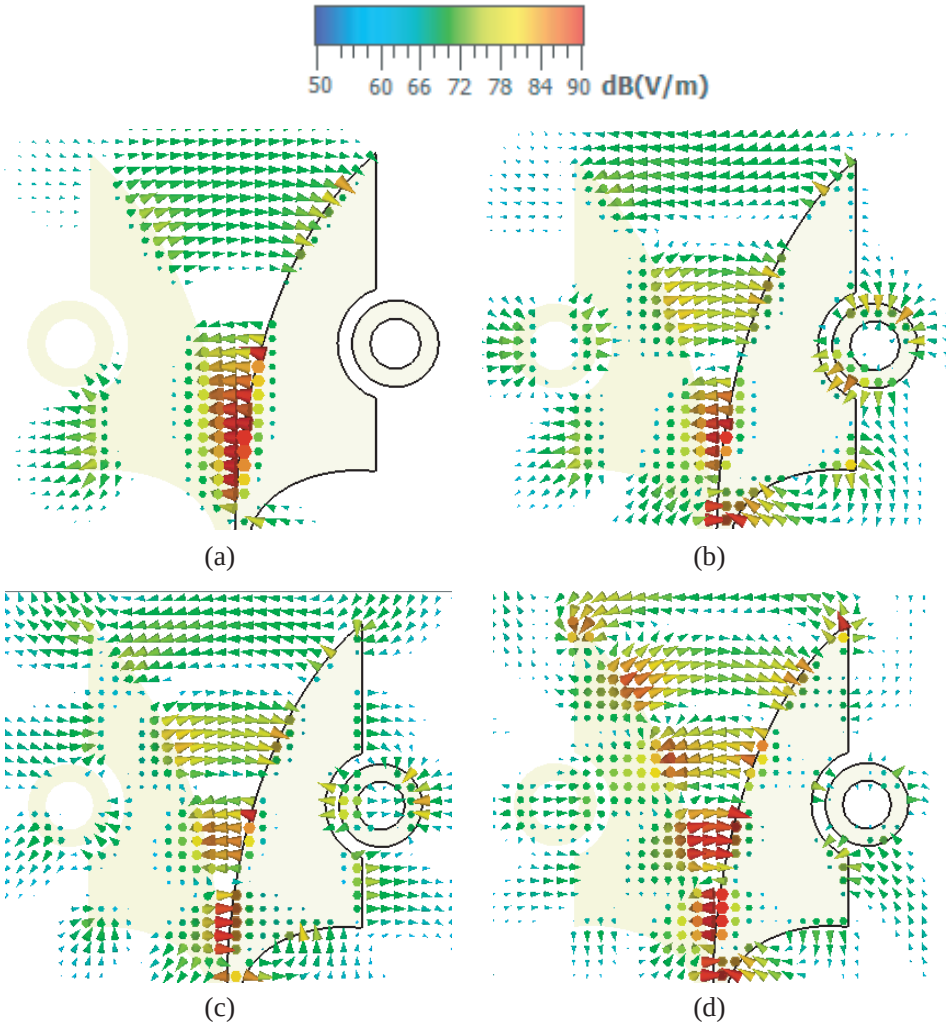

Figure 12. Electric field distributions in the tapered slot of the proposed Vivaldi antenna near the center frequencies of the four bands: (a) 25 GHz, (b) 35 GHz, (c) 45 GHz, and (d) 55 GHz. The dimensions of the antenna are listed in Table 1.

5. GAIN PATTERNS

The gain patterns produced by the proposed planar Vivaldi antenna near the center frequencies of the four frequency bands are presented in Figure 13. These patterns are obtained by the CST® simulator and correspond to the surface current distributions demonstrated in Figure 11 and the electric field

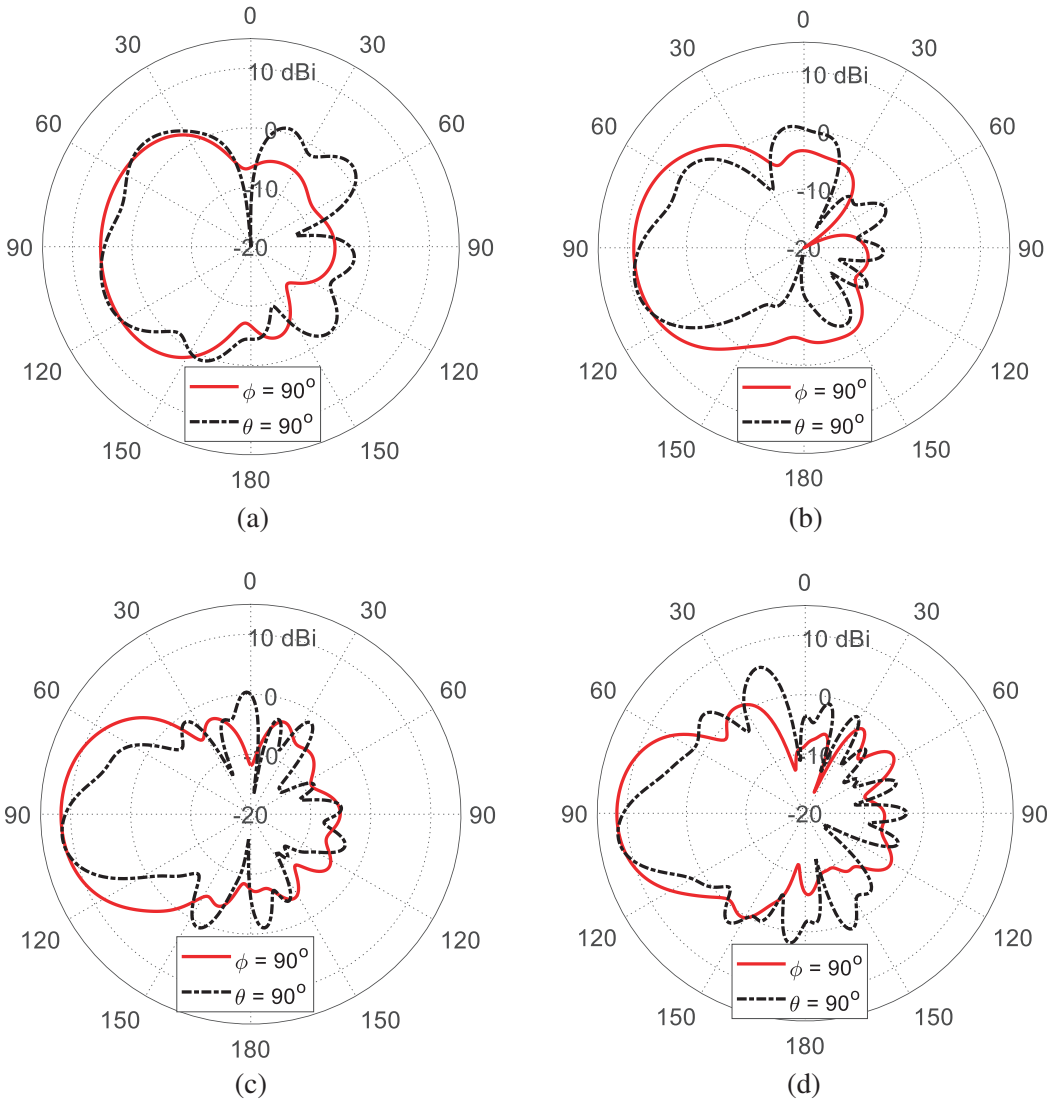

Figure 13. Gain patterns of the proposed Vivaldi antenna near the center frequencies of the four bands: (a) 25 GHz, (b) 35 GHz, (c) 45 GHz, and (d) 55 GHz.

Table 2. The maximum gain obtained at the center frequencies of the four bands of the proposed Vivaldi antenna.

Frequency (GHz)	Mode Order	Gain (dBi)
25	first	6.0
35	Second	9.0
45	Third	11.4
55	Fourth	12.0

distributions presented in Figure 12. The maximum gain obtained near the center frequencies of the four bands are listed in Table 2. It is shown that, like a multiband antenna, the gain of the proposed Vivaldi antenna increases with increasing the mode order. The maximum gain produced by this antenna is 12 dBi and is obtained at 55 GHz. The three-dimensional gain pattern obtained at 45 GHz (just for example) is presented in Figure 14.

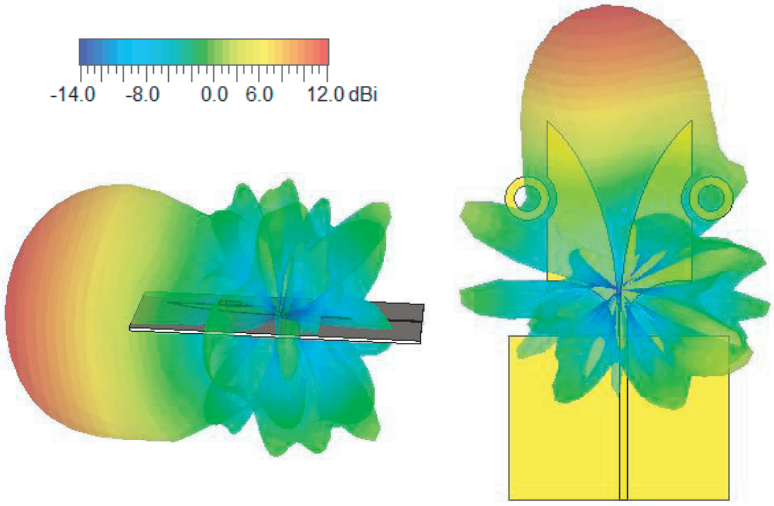

Figure 14. Two views of the three-dimensional gain pattern obtained by the proposed Vivaldi antenna at 45 GHz.

6. ANTENNA FABRICATION AND MEASUREMENTS

This section is concerned with describing the fabricated prototype of the proposed antenna and presenting the results of measurements for experimental assessment of its performance.

6.1. Antenna Fabrication

The proposed Vivaldi antenna is fabricated for investigating its performance through measurement. The antenna arms are printed on opposite faces of a Rogers' RO3003 substrate using the lithography technique. The fabricated antenna is presented in Figure 15 showing both the top and bottom faces. A coaxial launcher of the type 2.4 mm is used for feeding the antenna during measurements.

6.2. Measurements of the Reflection Coefficient at the Feeding Port

The measurement of the reflection coefficient at the input port of the fabricated model of the proposed Vivaldi antenna is presented in Figure 16. The Rohde and Schwartz VNA model ZVA67 is used for this purpose. The dependence of the reflection coefficient at the antenna feeding port on the frequency is depicted in Figure 17. The results of the simulation are compared to the measured response showing good agreement. It is shown that the proposed Vivaldi antenna has 50Ω-matched impedance over the four frequency bands: 22.0–27.7 GHz, 32.0–37.5 GHz, 41.5–46.6 GHz, and 51.7–56.7 GHz. The corresponding bandwidths are 5.7, 5.5, 5.1, and 5.0 GHz, respectively with percent bandwidths of 23%, 16%, 11.6%, and 9.2%, respectively. The four operable frequency bands are summarized in Table 3.

6.3. Measurement of the Radiation Pattern

For experimental validation of the simulation results concerned with the radiation pattern of the proposed Vivaldi antenna, the radiation pattern is measured at 45 GHz (just for example) in the two

(a) (b)

Figure 15. The fabricated model of the proposed Vivaldi antenna. (a) Top view. (b) Bottom view.

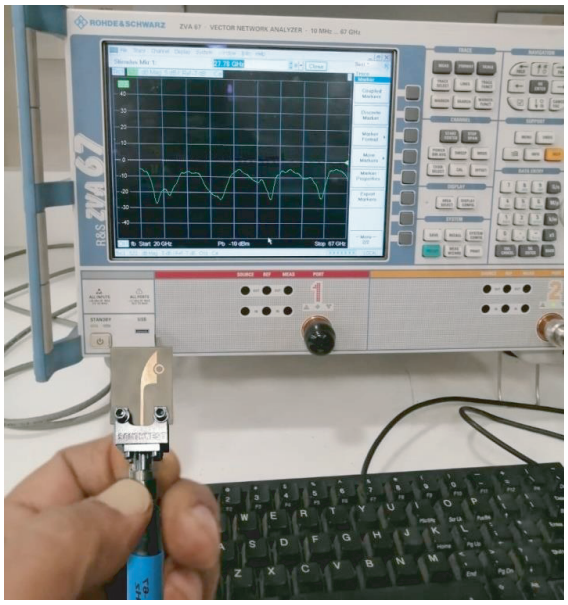

Figure 16. Measurement of the reflection coefficient at the feeding port of the Vivaldi antenna using the Rohde and Schwartz VNA model ZVA67.

Table 3. Impedance matching bandwidth for each of the four frequency bands of the proposed Vivaldi antenna.

Order of the Frequency Band	Frequency Band (GHz)	Bandwidth (GHz)	% Bandwidth
First	22.0–27.7	5.7	23%
Second	32.0–37.5	5.5	16%
Third	41.5–46.6	5.1	11.6%
Fourth	51.7–56.7	5.0	9.2%

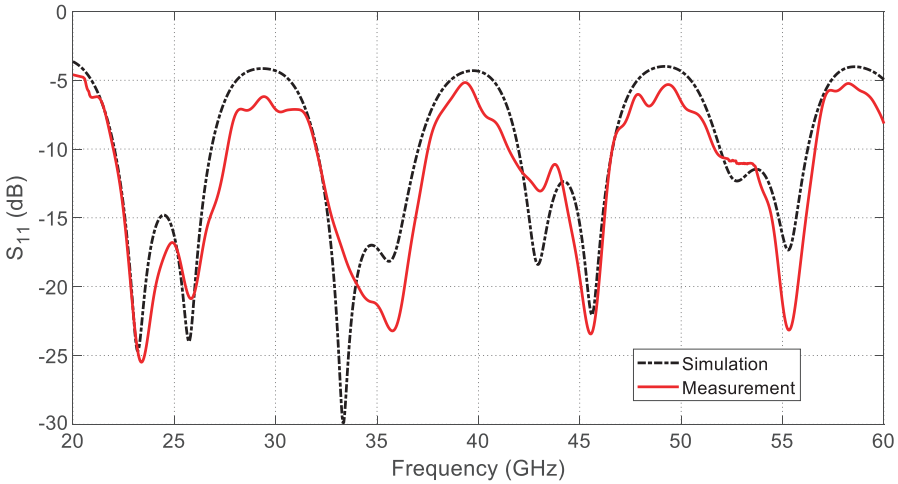

Figure 17. Frequency dependence of the magnitude of the reflection coefficient, $|S_{11}|$, at the antenna excitation port over the frequency band 20–60 GHz.

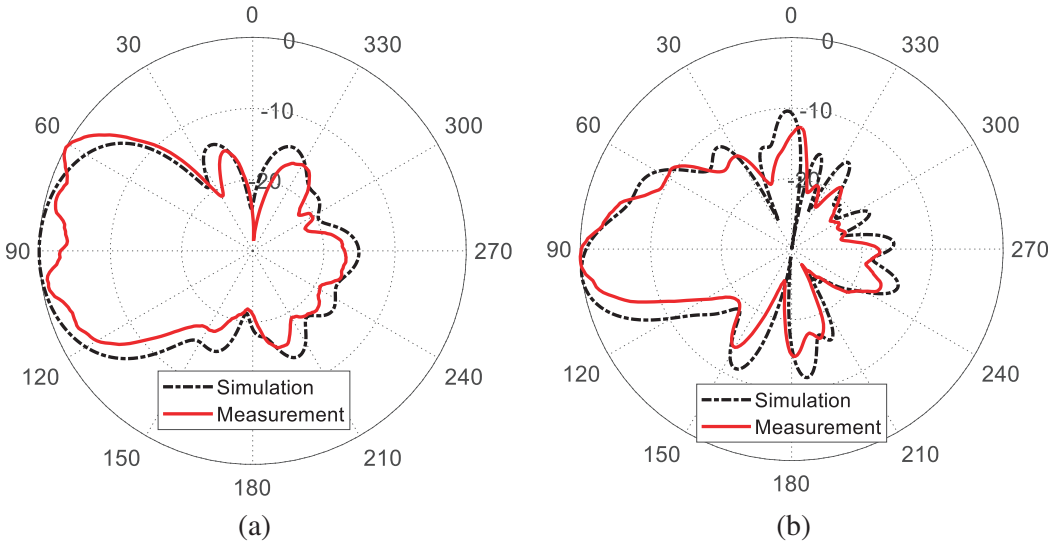

Figure 18. Radiation patterns for the proposed Vivaldi antenna obtained by simulation and measurement at 45 GHz in the planes (a) $\phi = 0°$ and (b) $\theta = 90°$.

planes $\phi = 0°$ and $\theta = 90°$. The radiation patterns obtained by simulation and measurement are depicted in Figure 18 showing good agreement.

6.4. Frequency Response of the Antenna Gain

The frequency response of the maximum gain obtained by the proposed Vivaldi antenna is presented in Figure 19. The antenna gain is measured following the method described in [20] and [21]. The experimental measurements show good agreement with the simulation results. It is shown that the maximum gain increases with increasing the frequency. The average values of the maximum gain over the first, second, third, and fourth frequency bands are about 6, 9, 11.4, and 12 dBi, respectively. Thus, like a multiband antenna, the gain of the proposed Vivaldi antenna increases with increasing the mode order of the near field.

The realized antenna gain is degraded over the frequency ranges of impedance-mismatch which are the frequency bands complementary to those listed in Table 3. Figure 20 presents a comparison

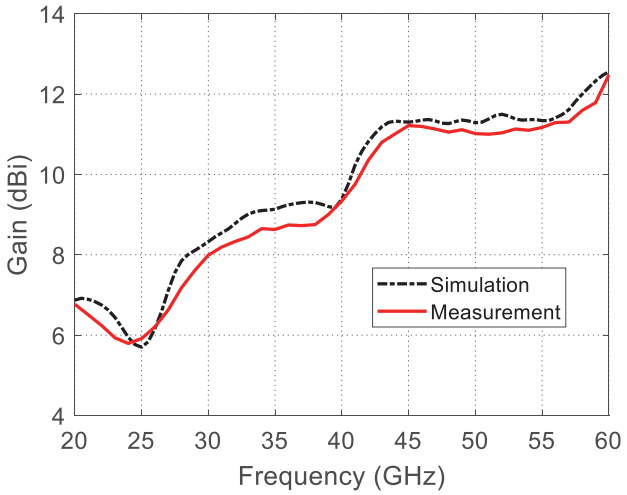

Figure 19. Frequency dependence of the gain of the proposed Vivaldi antenna over the entire frequency range (20–60 GHz).

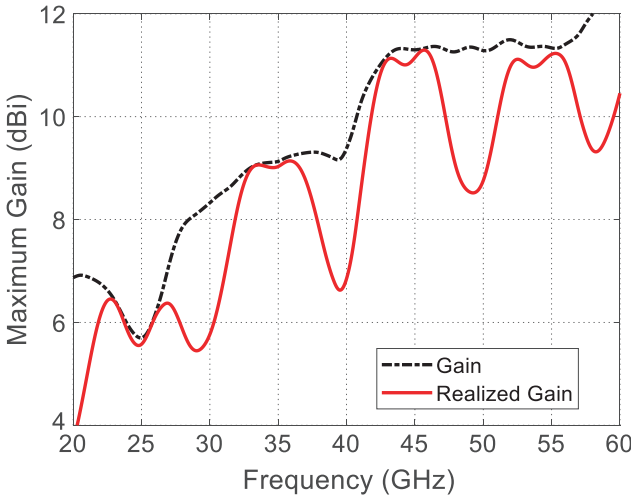

Figure 20. Frequency dependence of the gain in comparison to the realized gain of the proposed Vivaldi antenna over the entire frequency range (20–60 GHz).

between the gain and the realized gain over the entire frequency range (20–60 GHz). It is shown that the realized gain is degraded around the frequencies 20, 30, 40, 50, and 60 GHz, i.e., the realized gain is degraded outside the four bands for which the antenna is designed to operate.

6.5. Frequency Response of the Antenna Efficiency

The variation of the radiation efficiency of the proposed multiband Vivaldi antenna with varying the frequency is presented in Figure 21. The radiation efficiency is measured following the method described in [20] and [21]. The experimental measurements show good agreement with the simulation results. It is

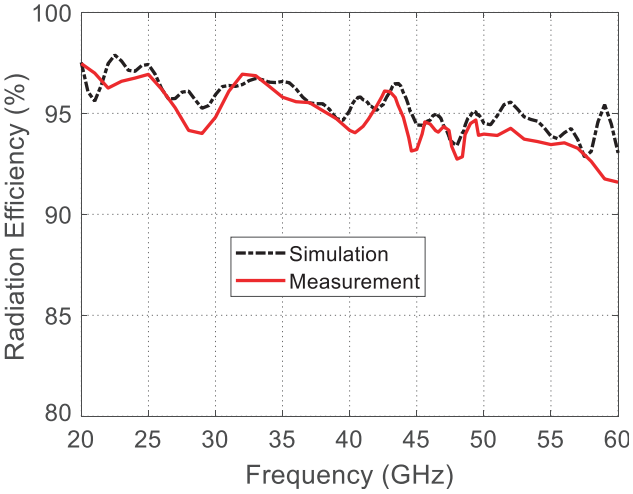

Figure 21. Frequency dependence of the radiation efficiency of the proposed Vivaldi antenna over the entire frequency range (20–60 GHz).

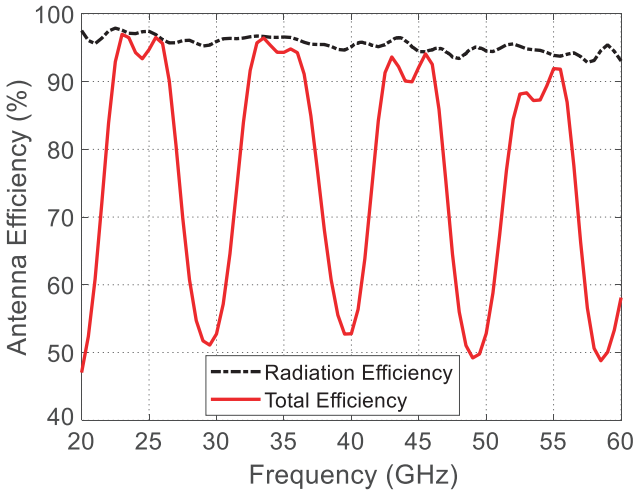

Figure 22. Frequency dependence of the radiation efficiency in comparison to the total efficiency of the proposed Vivaldi antenna over the the four frequency bands.

shown that the radiation efficiency decays with increasing the frequency with a very slow rate. However, the radiation efficiency is higher than 93% over all the operable frequency bands. This means that most of the power accepted at the antenna port is actually radiated to the far zone.

The total antenna efficiency is degraded over the frequency ranges of impedance-mismatch which are the frequency bands complementary to those listed in Table 3. Figure 22 presents a comparison between the total efficiency and the radiation efficiency over the entire frequency range (20–60 GHz). It is shown that the total efficiency is degraded around the frequencies 20, 30, 40, 50, and 60 GHz, i.e., the total efficiency is degraded outside the four bands for which the antenna is designed to operate.

7. SUMMARY AND COMPARISON WITH OTHER PUBLISHED WORK

The dimensions and the performance of the proposed Vivaldi antenna in comparison to other antennas proposed in some recent publication for operation in the millimeter range of the electromagnetic wave are summarized in Table 4. The presented performance measures are the frequency bands of operation, the bandwidth of impedance matching, maximum gain, and radiation efficiency.

The advantages of the proposed antenna design can be summarized as follows.

- The Vivaldi antenna proposed in the present work is the only antenna among those presented in the publications that can operate over four frequency bands for millimeter-wave applications with high gain and high radiation efficiency.
- Loading the antenna arms by parasitic rings through a semicircular slot is a novel method for gain enhancement of printed Vivaldi antennas.
- A novel microstrip line/parallel-strip line balun has been designed for wideband impedance matching.
- The proposed antenna has much smaller size than the other Vivaldi antennas presented in the recent publications to provide high gain and multiple frequency bands.

However, the following can be reported upon the comparisons listed in Table 4.

Table 4. List of comparative performance with other high-gain millimeter-wave printed Vivaldi antennas available in some recent publications.

Work	Dimensions (mm × mm × mm)	Frequency Band (GHz)	Bandwidth (GHz)	Maximum Gain (dBi)	Radiation Efficiency (%)
[4]	122 × 66 × 7.7	4.2–50	45.8	16	NA
[8]	6.67 × 3.2 × 0.133	24–30	6	13.8	98
[9]	66×110×1.575	6–26.5	20.5	9	NA
[10]	66 × 140 × 1.5	5.5–27	21.5	12	NA
[11]	50 × 66.4 × 1	4–30	26	5	NA
[19]	15 × 6 × 0.5	23.4–31 35.4–45	7.6 9.6	NA	88–98
[20]	90 × 40 × 0.508	3.4–40	36.6	14	NA
[22]	40 × 24 × 1.6	24.7–34.5	9.8	9.53	NA
[23]	45 × 20 × 0.8	4.2–45	40.8	11.4	NA
[Present]	23 × 17.9 × 0.25	22.0–27.7 32.0–37.5 41.5–46.6 51.7–56.7	5.7 5.5 5.1 5.0	9.0 10.2 11.4 12.0	98 97 95 93

- The Vivaldi antennas proposed in [8] and [19] are more compact than the antenna proposed in the present work.
- The Vivaldi antennas proposed in [8] and [20] have higher gain that of the antenna proposed in the present work.

8. CONCLUSION

The present work proposes a novel geometrical design of a compact Vivaldi antenna that is printed on the opposite faces of a thin dielectric substrate. It has been shown that the proposed antenna can operate as a quad-band antenna for millimeter-wave applications. To maximize the gain within a selected frequency band, each arm of the Vivaldi antenna is loaded by a ring-shaped parasitic element. The dimensions and location of the parasitic ring have been optimized to produce the maximum gain. The antenna has been fabricated and subjected to performance evaluation through measurements. The measurement show good agreement with the simulation results. It has been shown that the antenna impedance is matched over the four frequency bands: 22.0–27.7 GHz, 32.0–37.5 GHz, 41.5–46.6 GHz, and 51.7–56.7 GHz. The corresponding bandwidths are 5.7, 5.5, 5.1, and 5.0 GHz, respectively with percent bandwidths of 23%, 16%, 11.6%, and 9.2%, respectively. The corresponding values of the maximum gain are 6, 9, 11.4, and 12 dBi, respectively. Also, the corresponding values of radiation efficiency are 98%, 97%, 95%, and 93%, respectively. In spite of its compact size, the achieved gain is 12 dBi at 55 GHz and shows excellent stability over the entire frequency band that is selected for optimization. The novelty aspects of the proposed antenna design can be summarized as follows. The Vivaldi antenna proposed in the present work is the only antenna among those presented in the publications that can operate over four frequency bands for millimeter-wave applications with high gain and high radiation efficiency. Loading the antenna arms by parasitic rings through a semicircular slot is a novel method for gain enhancement of printed Vivaldi antennas. A novel microstrip line/parallel-strip line balun has been designed for wideband impedance matching. The proposed antenna has much smaller size than the other Vivaldi antennas presented in the recent publications to provide high gain and multiple frequency bands.

REFERENCES

1. CihatŞeker, M. T. G. and T. Ozturk, "A review of millimeter wave communication for 5G," *2nd International Symposium on Multidisciplinary Studies and Innovative Technologies (ISMSIT)*, 2018.
2. Chittimoju, G. and U. D. Yalavarthi, "A comprehensive review on millimeter waves applications and antennas," *Journal of Physics: Conference Series*, Vol. 1804, No. 1, 012205, IOP Publishing, 2021.
3. Kadiyam, S. and A. J. Rani, "Design and analysis of a high gain millimeter-wave antenna array for dual purpose applications," *Wireless Personal Communications*, Vol. 130, No. 1, 593–607, 2023.
4. Bhattacharjee, A., A. Bhawal, A. Karmakar, and A. Saha, "Design of an antipodal Vivaldi antenna with fractal-shaped dielectric slab for enhanced radiation characteristics," *Microwave and Optical Technology Letters*, Vol. 62, No. 5, 2066–2074, 2020.
5. Gibson, P., "The Vivaldi aerial," *9th European Microwave Conference*, Vol. 1, 101–105, 1979.
6. Gazit, E., "Improved design of the Vivaldi antenna," *IEE Proceedings H — Microwaves, Antennas and Propagation*, Vol. 135, 89–92, 1988.
7. Karmakar, A., A. Bhattacharjee, A. Saha, and A. Bhawal, "Design of a fractal inspired antipodal vivaldi antenna with enhanced radiation characteristics for wideband applications," *IET Microwaves, Antennas & Propagation*, Vol. 13, No. 7, 892–897, 2019.
8. Dixit, A. S. and S. Kumar, "Gain enhancement of antipodal Vivaldi antenna for 5G applications using metamaterial," *Wireless Personal Communications*, Vol. 121, No. 4, 2667–2679, 2021.
9. Bang, J., J. Lee, and J. Choi, "Design of a wideband antipodal Vivaldi antenna with an asymmetric parasitic patch," *Journal of Electromagnetic Engineering and Science*, Vol. 18, No. 1, 29–34, 2018.

10. Nassar, I. T. and T. M. Weller, "A novel method for improving antipodal Vivaldi antenna performance," *IEEE Transactions on Antennas and Propagation*, Vol. 63, No. 7, 3321–3324, 2015.
11. Teni, G., N. Zhang, J. Qiu, and P. Zhang, "Research on a novel miniaturized antipodal Vivaldi antenna with improved radiation," *IEEE Antennas Wireless Propag. Lett.*, Vol. 12, 417–420, 2013.
12. Vinci, G. and R. Weigel, "Multiband planar vivaldi antenna for mobile communication and industrial applications," *2010 International Conference on Electromagnetics in Advanced Applications*, 93–96, IEEE, 2010.
13. Indira, N. D., B. T. P. Madhav, K. Balaji, B. Rajagopalarao, and V. K. Kishore, "Multiband Vivaldi antenna for X and Ku band applications," *International Journal of Advanced Networking and Applications*, Vol. 3, No. 5, 1375, 2012.
14. Kumar, R. and S. Priyadarshi, "Multi-band Vivaldi antenna for wireless communication: Design, analysis and modelling of vivaldi antenna," *2016 International Conference on Communication and Electronics Systems (ICCES)*, 1–4, IEEE, 2016.
15. Kapoor, A., P. Kumar, and R. Mishra, "High gain modified Vivaldi vehicular antenna for IoV communications in 5G network," *Heliyon*, Vol. 8, No. 5, 2022.
16. Ameen, J. J. H., "Design and simulation of multi-band M-shaped Vivaldi antenna," *Intelligent Systems Design and Applications: 17th International Conference on Intelligent Systems Design and Applications (ISDA 2017) held in Delhi, India, December 14–16, 2017*, 903–912, Springer International Publishing, 2018.
17. Chagharvand, S., M. R. Hamid, M. R. Kamarudin, and J. R. Kelly, "Wide and multi-band reconfigurable Vivaldi antenna with slot-line feed," *Telecommunication Systems*, Vol. 65, 79–85, 2017.
18. Selvaraj, D., R. Priyadarshini, S. Sharon Hephzibah, S. Vaishnavi, B. K. Tanmae, and M. Yuvashree, "Design of Triband Vivaldi antenna for UWB application," Vol. 6, Issue III, March 2018, available at www.ijraset.com.
19. Dixit, A. S. and S. Kumar, "A dual band antipodal Vivaldi antenna for fifth-generation applications," *2021 IEEE Indian Conference on Antennas and Propagation (InCAP)*, 224–227, IEEE, 2021.
20. Yassin, M. E., K. F. A. Hussein, Q. H. Abbasi, M. A. Imran, and S. A. Mohassieb, "Flexible antenna with circular/linear polarization for wideband biomedical wireless communication," *Sensors*, Vol. 23, No. 12, 2023.
21. Fouad, M. S., A. E. Farahat, K. F. A. Hussein, A. H. A. Shaalan, and M. F. Ahmed, "Super-wideband fractal antenna for future generations of wireless communication," *Progress In Electromagnetics Research C*, Vol. 136, 137–149, 2023.
22. Dixit, A. S. and S. Kumar, "The enhanced gain and cost-effective antipodal Vivaldi antenna for 5G communication applications," *Microwave and Optical Technology Letters*, Vol. 62, No. 6, 2365–2374, 2020.
23. Dixit, A. S. and S. Kumar, "A wideband antipodal Vivaldi antenna," *2021 7th International Conference on Signal Processing and Communication (ICSC)*, 11–14, IEEE, 2021.